

# Engineered Nanofluidic Preconcentration Devices by Ion Concentration Polarization

Seok Young Son<sup>1</sup>, Sangjun Lee<sup>1</sup>, Hyomin Lee<sup>1,2</sup> & Sung Jae Kim<sup>1,3,4,\*</sup>

Received: 09 January, 2016 / Accepted: 02 February, 2016 / Published online: 29 April, 2016  
© The Korean BioChip Society and Springer 2016

**Abstract** A nanofluidic preconcentration device utilizing an ion concentration polarization (ICP) phenomenon has been regarded as one of the most efficient mechanism for preconcentrating low abundant molecules to be detected. In this review, a short fundamental aspect behind ICP was introduced and detailed engineering endeavors to enhance the performance of the preconcentration device were followed. While a conventional nanostructure based on silicon or glass substrate lose its ion-selectivity at a physiologically relevant electrolyte concentration, Nafion as a highly charged nanoporous material would maintain its permselectivity at the concentration so that various fabrication processes utilizing Nafion were introduced. In order to extend the capability of the device in terms of preconcentration factor and throughput, dual gates, “U”-shaped and one-channel device were shown with their *pros* and *cons*. Last section would introduce the most recent development of preconcentration mechanism; the simultaneous preconcentration with separation, the radial preconcentration and the two stress-free preconcentration mechanisms. Conclusively, this review would not only provide the key insight of development history of the nanofluidic preconcentration device but also contribute for creating the next generation preconcentration mechanisms.

**Keywords:** Nanofluidics, Nano-electrokinetics, Ion concentration polarization, Analyte preconcentration, Nano-fabrication

## Introduction

Miniaturized analytical tools in biomedical fields and environmental applications have been extensively researched over last couple of decades with the aid of the advances in micro- and nano-fabrication techniques<sup>1-3</sup>. These groundbreaking tools rapidly has changed the main scope of such application fields, since it provided numerous outstanding advantages over laboratory-scaled tools such as fast reaction time, minimal consumptions of priceless samples and a maximized scalability for portable platforms. However, the operation with minimum volume of samples often demanded a detector that has the extremely low limit of detection (LOD), if the samples contained low abundant molecules such as early-stage cancer biomarkers and heavy metals which caused serious diseases even at an immensely low concentration<sup>4,5</sup>. While the detectors, an inductively coupled plasma mass spectrometry and a Matrix Assisted Laser Desorption/Ionization (MALDI) for examples, could satisfy such LOD, their large volume and high cost would prohibit the advances toward a ubiquitous era. Instead, numerous methods of preconcentrating such low abundant molecules have been developed for substituting the traditional analytical tools. Physical micro- or nano-filtrations were the simplest method, but inherent clogging issues and low recovery efficiency seriously delayed the development of practical applications. Recently, several electrokinetic phenomena were suggested for new preconcent-

<sup>1</sup>Department of Electrical and Computer Engineering, Seoul National University, Seoul 08826, Korea

<sup>2</sup>Institute of Advanced Machines and Design, Seoul National University, Seoul 08826, Korea

<sup>3</sup>Big Data Institute, Seoul National University, Seoul 08826, Korea

<sup>4</sup>Inter-university Semiconductor Research Center, Seoul National University, Seoul 08826, Korea

\*Correspondence and requests for materials should be addressed to S.J. Kim (✉ gates@snu.ac.kr)

tration mechanisms such as capillary electrophoresis<sup>6</sup>, microfluidic field-amplified sample stacking<sup>7</sup>, isotachopheresis<sup>8</sup> and isoelectric focusing<sup>9</sup>, *etc.*

More recently, micro/nanofluidic preconcentration device based on an ion concentration polarization (ICP) phenomenon that was firstly reported in 2005 has drawn a striking attention, due to its high preconcentration factor up to a million-fold and easy operation<sup>10</sup>. ICP is a unique electrochemical phenomena that occurs near a nanoporous membrane (or nanochannel) under dc electrical bias<sup>11</sup>. When the membrane immersed in an electrolyte solution, it should have a surface charge on it. Considering one nanopore in the membrane, the surface charge on one side of pore wall can influence the other side of pore wall due to its nanometer scale so that the nanopore acts as the barrier against co-ions in the solution. Therefore, only counter-ions can pass through the nanopore, while co-ions are rejected from the nanopore. This phenomena is known as perm-selectivity or ion-selectivity. Since the most of membrane materials have a negative surface charge, it acts as cation-selective membrane. Under dc bias, the electrolyte concentration at the anodic side of membrane decreases and finally reaches near-zero concentration to form an ion depletion zone, while the concentration at the cathodic side enriches to form an ion enrichment zone, *i.e.* the ionic concentration is polarized at both sides of membrane<sup>12</sup>. This is the representing phenomenon of ICP.

The ion depletion zone has arisen numerous fundamental issues in nanoscale electrokinetics such as instability<sup>13-15</sup>, overlimiting current<sup>16-18</sup> and nonlinear electrokinetic flows<sup>19,20</sup>, but their details would be omitted in this review, since they are out of scope. Briefly, the near-zero electrolyte concentration inside the ion depletion zone led to a locally high electrical resistance and amplified the local electrokinetic flow inside the zone<sup>20</sup>. In order to mass conservation, the amplified electrokinetic flow forms as a fast vortical motion that has never been achieved with 1<sup>st</sup> kind of electroosmotic flow. In addition to this, the electro-neutrality should be satisfied inside the ion depletion zone. The combined effects of these two factors, *i.e.* strong vortical motion and electro-neutrality, let the ion depletion zone act as an electrical filter only for charged molecules. Thus, any charged molecules regardless of their polarity should be accumulated at the outer-boundary of the ion depletion zone and their concentrations locally increased up to a million-fold. This is the mechanism of nanofluidic preconcentration device. Compared to aforementioned mechanism such as isotachopheresis, ICP preconcentrator has higher preconcentration factor because the target molecules were continuously

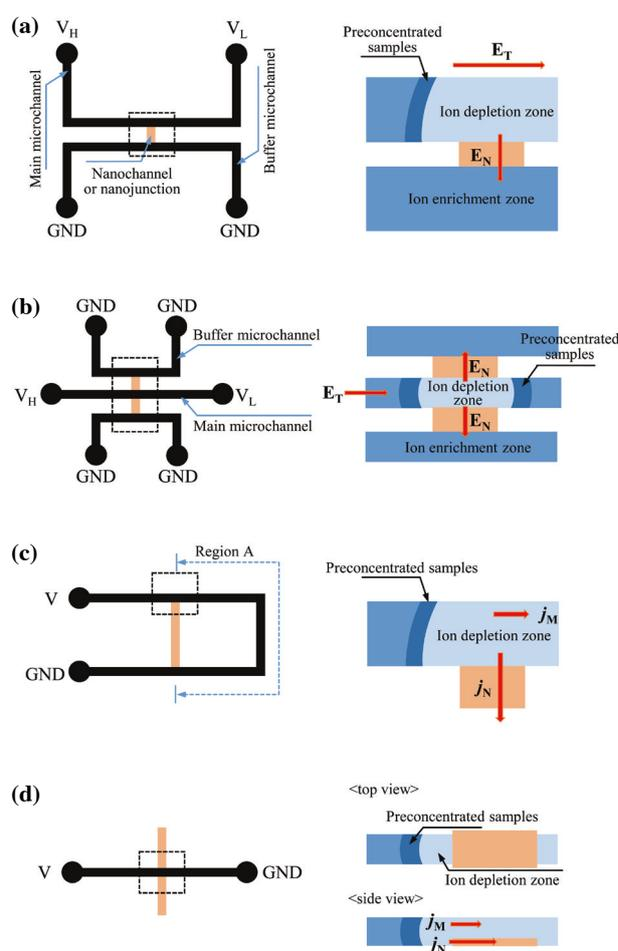


**Figure 1.** Schematic illustrations of the preconcentration device and the mechanism of ICP in (a) H-shaped device, (b) dual gates device, (c) U-shaped device and (d) one-channel device.  $V_H$  and  $V_L$  were applied electric potentials of high and low to induce a tangential electrical field ( $E_T$ ).  $E_N$  was a normal electric field across the nanojunction or the nanochannel.  $j_M$  and  $j_N$  were cation fluxes across a microchannel and the nanojunction, respectively. Left column was a magnified view from the dashed square of the right column.

supplied from reservoir that could be considered as infinite volume compared to the volume of microchannel. Despite of these fruitful advantages, there were still several inherent limitations in the ICP mechanism. Most importantly, an “H”-shaped structure that required four voltage inputs hampered a practical utility as shown in Figure 1(a), since extremely complex electrode connections required for the multiplex version of the preconcentration device. The locally preconcentrated sample inside microchannel had a volume from few pico- to nano-liters so that increasing a throughput or interfacing with downstream devices were challenging. In addition, ICP would be diminished with in-

creasing the bulk electrolyte concentration, since the conductivity ratio of bulk solution to electrolytes inside nanopore would not be enough to provide the perm-selectivity of the membrane or nanochannel<sup>21,22</sup>.

In this review, engineering endeavors to overcome these limitations in the last decade were profoundly introduced. Highly charged membrane material and its fabrication process, the efficient microchannel structures for simplifying the electrical connections, and finally, new types of preconcentration mechanism would be summarized with their *pros* and *cons* so that this review will play a guidance role for whom not only started to explore nanofluidic preconcentration mechanism itself but also had researched ICP applications such as a bioanalytical sensing or environmental monitoring field.

## Highly Charged Nanoporous Materials

Typical materials that used for the substrate of nanochannel were silicon wafer or glass, but their surface charges were relatively low (Si wafer: 25-50 mC/m<sup>2</sup> and glass: <13 mC/m<sup>2</sup>)<sup>23,24</sup>. With such materials, the nanochannel lost its perm-selectivity with high electrolyte concentration. For example, 3 mM and 15 mM were reported as a maximum electrolyte concentration that can initiate ICP with glass<sup>25</sup> and silicon<sup>12</sup> substrate, respectively. However, a practical solution for conventional biological experiments has an electrolyte concentration over 150 mM and even 500 mM of seawater sample was used in environmental monitoring field. In order to sustain a perm-selectivity at such high concentration, the surface charge of nanochannel or nanoporous membrane should be much higher than the typical material<sup>21</sup>. In addition, the fabrication processes involving such materials always required high-cost lithographical processes so that a low surface charge and a high fabrication cost were nuisances for practical utilities of ICP application. Compared to these materials, Nafion recently appeared to be an alternative material for the perm-selective membrane. Nafion is a highly charged sulfonated tetrafluoroethylene (Teflon) based fluoropolymer-copolymer (the surface charge of 200-600 mC/m<sup>2</sup>)<sup>26</sup> and has received a considerable attention as a proton conductor for proton exchange membrane (PEM) fuel cells<sup>27,28</sup>. Pores allow movement of cations but the membranes do not conduct anions or electrons. Since various types of Nafion such as powder, solution and sheet has been already commercialized so that a fabrication process involving Nafion required only soft-lithographical method, leading to the Nafion for a versatile material in the nanofluidic applications. Self-

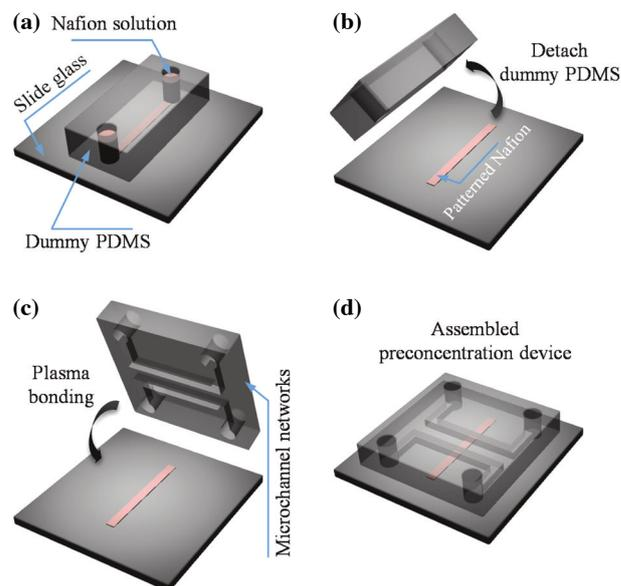


**Figure 2.** Fabrication steps of the surface patterning method using Nafion solution.

sealed method utilized the flexibility of PDMS<sup>29</sup>. A razor-cut trench was filled with Nafion solution so that the nanoporous membrane formed vertically inside PDMS substrate. By flowing Nafion solution through densely packed microparticles, thick nanoporous membrane was able to be integrated with deep microchannels<sup>30,31</sup>. Among those innovative methods, a surface patterning method<sup>32</sup> has become one of most favorite fabrication method. The schematic procedures were described in Figure 2. Like a stamping method, a dummy microchannel was introduced to guide the Nafion solution so that the patterned Nafion can follow the shape of the microchannel (Figure 2(a)). By removing the dummy microchannel, bottom substrate (usually slide glass) was able to have a designated Nafion pattern after heating at 95°C for 5 minutes (Figure 2(b)). Then desired PDMS microchannel networks would be connected by plasma bonding between the PDMS piece and the glass slide (Figure 2(c)). While the surface patterning method would connect microchannels and nanoporous membrane only at the bottom of microchannels and it was inappropriate in the case that required aggressive chemical treatments on the glass slide, the easiness of fabrication and the versatile shape of Nafion nanojunction would encourage one to adapt this method. Therefore, the high conductivity of Nafion and the easy fabrication method using it would accelerate the researches of nanofluidic applications, especially with ICP phenomenon. As followed, numerous biological experiments with 1X PBS (~150 mM)

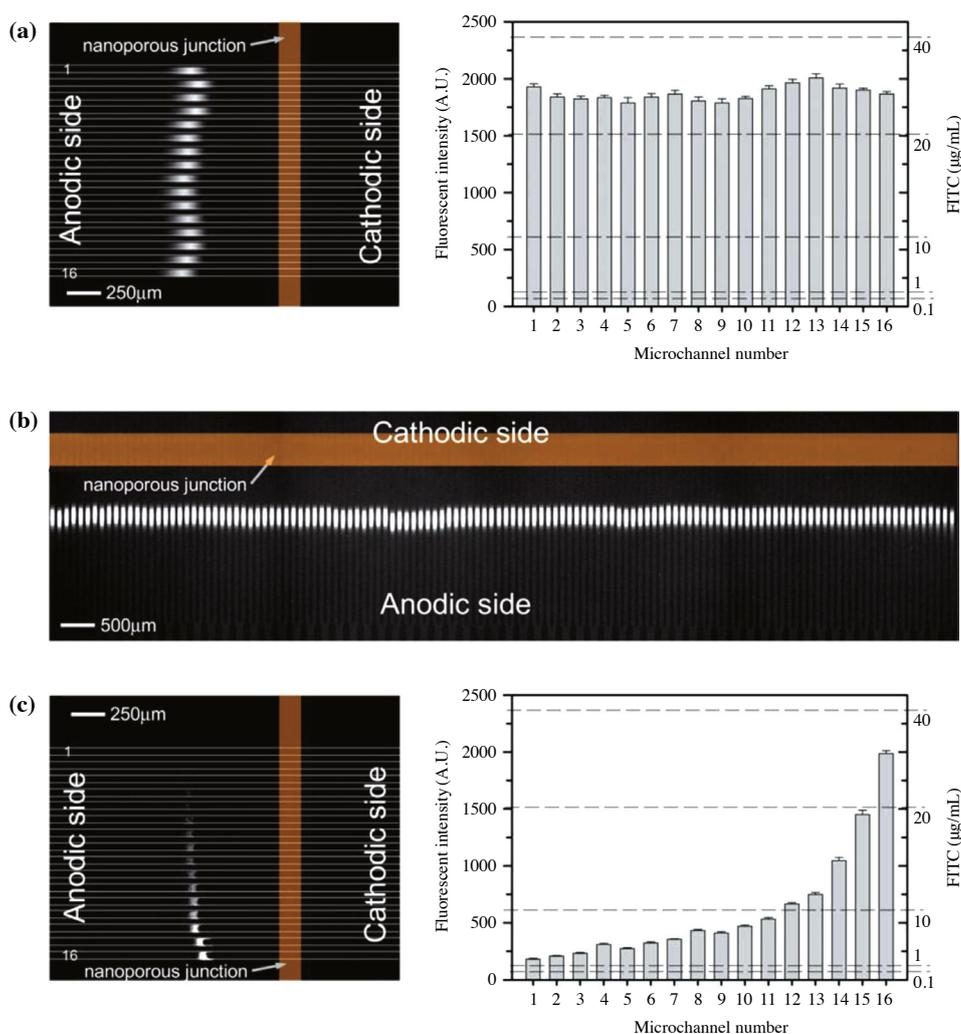


**Figure 3.** (a) The operation of the same length device (16-channel) and the fluorescent intensity plot for showing the same concentration factor. (b) The fluorescent image of 128-channel multiplexed concentration device. (c) The operation of serial preconcentration with a different length device (16-channel) and the fluorescent intensity plot showing the channel length dependency of concentration factor. Reproduced by permission of The Royal Society of Chemistry<sup>36</sup>.

buffer solution<sup>33</sup> and seawater (~500 mM) desalination<sup>34</sup> using Nafion junction were successfully demonstrated.

## Efficient Microchannel Networks

### Dual Gates Preconcentration Device

As described, conventional “H”-shaped preconcentration devices have been fabricated using silicon and glass nanochannels. As shown in Figure 1(a), its configuration was that two parallel microchannels were connected with the nanochannels at the center of microchannels. Thus, the ion depletion zone was formed

from the bottom of the main microchannel as shown in the second image of Figure 1(a). In such case, the repulsive force was uneven vertically along the microchannel height. A dual gates device had a configuration that one main microchannel were surrounded by two ground microchannel and the nanochannels connected them at the center of microchannels as shown in Figure 1(b). Then, the repulsive force was more uniform along the vertical line in the center microchannel than the “H”-shaped device. It was reported that the preconcentration factors with the dual gates device were higher than that with “H”-shaped device<sup>35</sup>. However, the dual gates design still have limitation of complex electrical connections.

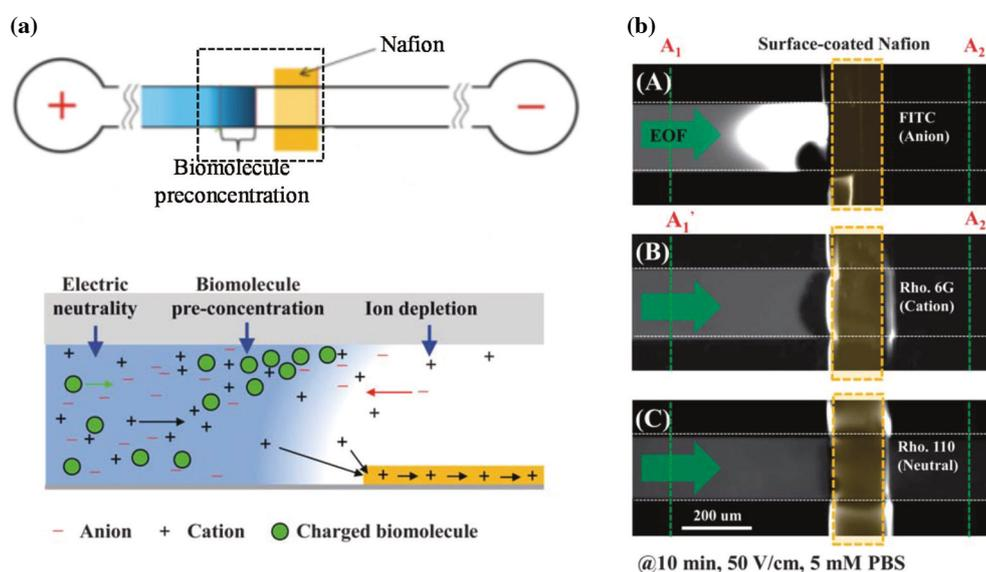


**Figure 4.** (a) The surface-patterned Nafion film acted as a selective ion transporter in the presence of an electric-field, so an ion depletion zone developed near and above the Nafion film. The illustration of the ICP phenomenon by the Nafion film that rapidly and selectively absorbed, transported, and discharged cations from the anodic side to the cathodic side, resulting in the local formation of the ion depletion zone. (b) (A) Negatively charged dye molecules, FITC, in 5 mM PBS buffer cannot penetrate the ion depletion zone. (B) Positively charged dye molecules, Rhodamine 6G, in the same buffer were initially blocked by the ion depletion zone but the ratio suddenly increases up to the same level as the neutral dye. (C) More than 30% of the neutral dye molecules, Rhodamine 110, pass over the Nafion film. Reproduced by permission of The Royal Society of Chemistry<sup>39</sup>.

### U-shaped Preconcentration Device

After the surface patterning method using Nafion material was introduced, its design flexibility was able to accelerate the development of engineered nanofluidic preconcentration device. The first variation was “U”-shaped preconcentration device<sup>36</sup>. As shown in Figure 1(c), there was only one u-turned microchannel and the electrical voltages were applied at each end of microchannel. The design rule was governed by the conductivity ratio of Nafion nanojunction to the portion of u-turned microchannel (denoted as region A in Figure 1(c)). The total length and cross-sectional area of region A, the bulk electrolyte concentration and the locations of Nafion nanojunction would determine the path of cation flux. If the ion flux through Nafion ( $j_N$ ) was more favorable (or similar) than the region A ( $j_M$ ), *i.e.*  $j_M < j_N$ , ICP was triggered. More importantly, the U-shaped devices were also easily extended to the multiplexed version<sup>36</sup>, since it only required one voltage input and one ground regardless of number of multiplexed microchannel. As shown in Figure 3, a massive multiplexed device with 16 and 128 microchannels at the same preconcentration factor and the serial preconcentration ratio were successfully demonstrated. In addition, this design was also utilized as micromixer<sup>37</sup>, since a sample flow was vigorously agitated and re-

combined again with strong tangential force along the microchannel.

### One-channel Preconcentration Device

More advanced design than “U”-shaped device was a straight channel device or one-channel device. In a straight microchannel, the conducting Nafion was patterned at the bottom of the microchannel and an electrical potential / an electric ground were applied at each end of microchannel as shown in Figure 1(d). If the cation flux through a Nafion pattern ( $j_N$ ) was larger than through bulk flow above the Nafion pattern ( $j_M$ ) (since the conductivities of Nafion and the sample above the Nafion were different), ICP was triggered at the anodic end of Nafion pattern. This one-channel device excluded any variation of microchannel layout and, thus, this has been considered as the simplest microchannel design that had ever been reported (Figure 4)<sup>38,39</sup>. Also the multiplexed version of one-channel device was demonstrated as well<sup>40</sup>. Traditional nanochannels fabricated by e-beam or DRIE were not appropriate for the one-channel device, because those nanochannels were incapable of transporting counter-ion in such open environment, *i.e.* the conventional nanochannel should “connect” the microchannels by being buried inside building block, but the one-channel device had the

nanojunction inside the microchannel. Note that 1-dimensional micro-nano-microchannel connected device was incapable of preconcentrating analytes, since there was no continuous inflow of the analyte in the device. Furthermore, since the conductivity of Nafion is similar as that of electrolyte solution at 1 M concentration, one can initiate ICP with most of physiological sample concentration range. However, both U-shaped device and one-channel device had a disadvantage in terms of power consumption, since excess ionic currents should flow even in low conductivity zone, *i.e.* the region A of U-shaped device and the upper part of Nafion in one-channel device.

## New Types of Nanofluidic Preconcentration Device

### Simultaneous Separation and Preconcentration for Multiple Analytes

The basic concept of nanofluidic preconcentration device was that creating an electrical barrier by strong convective fluid flows and electroneutrality. Thus, it had been considered all of charged molecules could be accumulated at the outer-boundary of the ion depletion zone. Later on, this turned to be not always true. With a proper voltage configuration to apply a moderate tangential electrical field, multiple analytes would be preconcentrated and separated simultaneously<sup>41-43</sup>. Since the physicochemical properties of each analytes had their unique values, the locations where the external forces were balanced out should be different. The drag forces and the electrophoretic forces were involved in the ICP preconcentration and their deterministic parameters were a size of molecules and an electrical

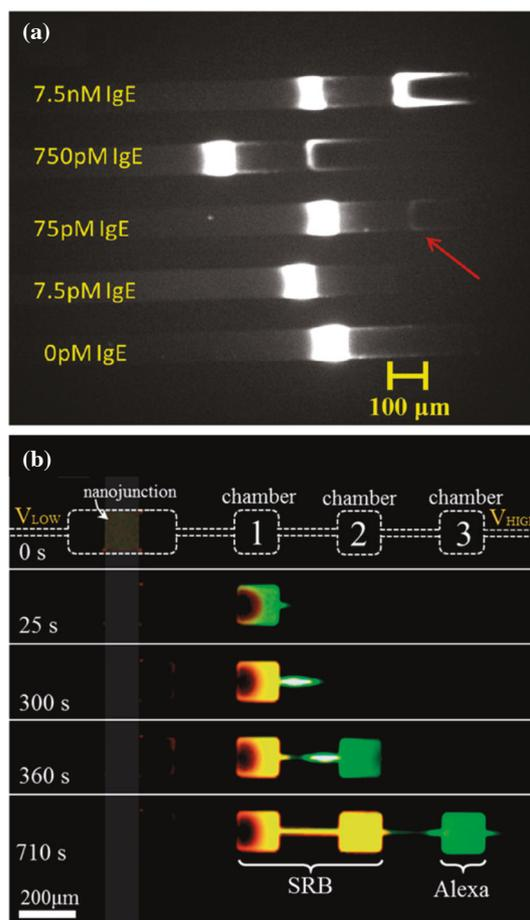


**Figure 5.** (a) The concentration-enhanced aptamer affinity probe electrophoresis assay for the detection of IgE. Reprinted with permission<sup>41</sup>. Copyright 2011 American Chemical Society. (b) Time-lapse images of selective preconcentration of sulfur rhodamine B (SRB) and Alexa fluor 488. Reproduced by permission of The Royal Society of Chemistry<sup>43</sup>.

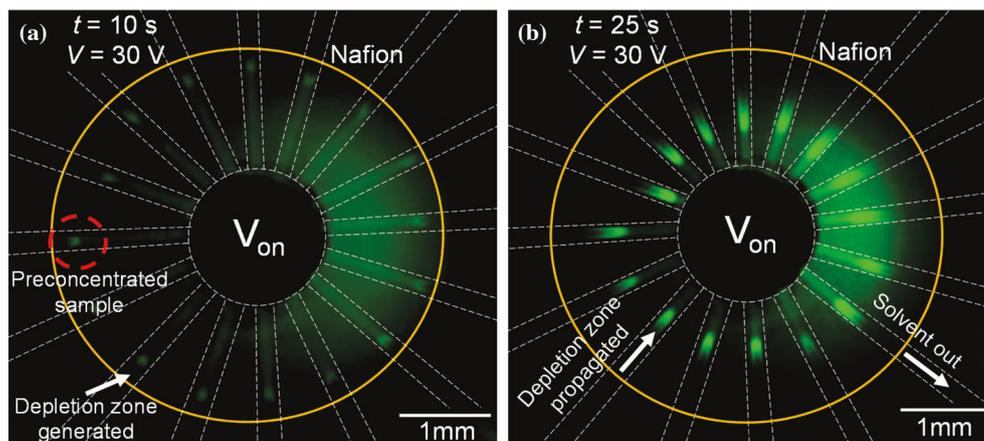


**Figure 6.** The fluorescent dye migration during an operation of radial preconcentrator. (a) A depletion zone generated inside the Nafion circle. (b) The preconcentrated plugs were migrated toward the center.

charge on it. Thus, they should have designated locations to be preconcentrated. Using this mechanism, several studies were reported to demonstrate the simultaneous operation of separation and preconcentration of multiple analytes. Cheow *et al.* reported an aptamer-protein complex and a free aptamer were simultaneously separated and preconcentrated at different location due to their size and charge difference (Figure 5(a))<sup>41</sup>. They utilized the device as a detector for whether an aptamer was reacted or not. Recently, Choi *et al.* employed the simultaneous separation and preconcentration device combined with pneumatic valves so that the device enabled to operate the three basic operations of analytical chemistry in a single platform, *i.e.* separation, preconcentration and sample extraction (Figure 5(b))<sup>43</sup>.

### Radial Preconcentration Device

While various multiplexed scheme had been introduced, one of preferred platform was a radially networked preconcentration device. The multiple connections of

each microchannel shared one output reservoir so that the preconcentrated samples were collected into the outlet. With an “H”-shaped preconcentration device, only half radial preconcentrator was demonstrated due to extremely complex electrical connections<sup>32</sup>. Later on, the repeated radial connections of micro- and nano-channel enabled to obtain an 800-fold preconcentration factor for 1 hour operation<sup>44</sup>, but this scheme utilized the ion enrichment zone so that the factor was lower than previously reported “H”-shaped device.

Since the one-channel device enabled to setup the preconcentration device with minimal number of electrical connections, the design was easily expanded to the radial preconcentration device. As shown in Figure 6, a circular Nafion junction was patterned at a designated radius so that the target molecules from the inlet at the center of the nanojunction would be trapped inside the circle of nanojunction with an external voltage input. After the preconcentration process, the preconcentrated samples from each microchannel would be easily recovered from the inlet reservoir.

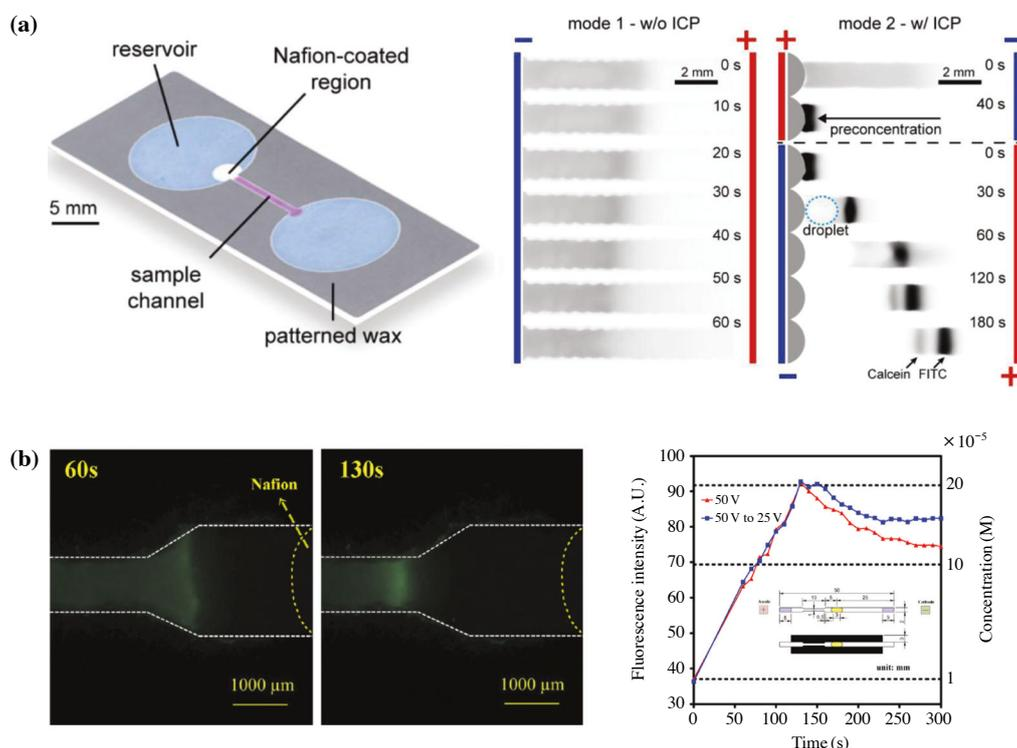


**Figure 7.** (a) The schematics of the paper-based preconcentration device with reservoirs (blue), sample channel (purple), and Nafion-coated region (white). Left images showed that preconcentration and separation in the paper-based ICP device with and without ICP. Reprinted with permission<sup>49</sup>. Copyright 2015 American Chemical Society. (b) Fluorescence images captured in optimal convergent-channel paper-based device at 60 s and 130 s after applying external potential of 50 V. The images show the enhancement of concentration by the geometric effect. The plot showed the variation of fluorescence intensity and sample concentration over time in optimal convergent-channel paper-based device given constant potential of 50 V for 300 s or potential of 50 V for 130 s and reduced potential of 25 V for the remainder of the concentration period. Reprinted with permission<sup>50</sup>. Copyright 2015, AIP Publishing LLC.

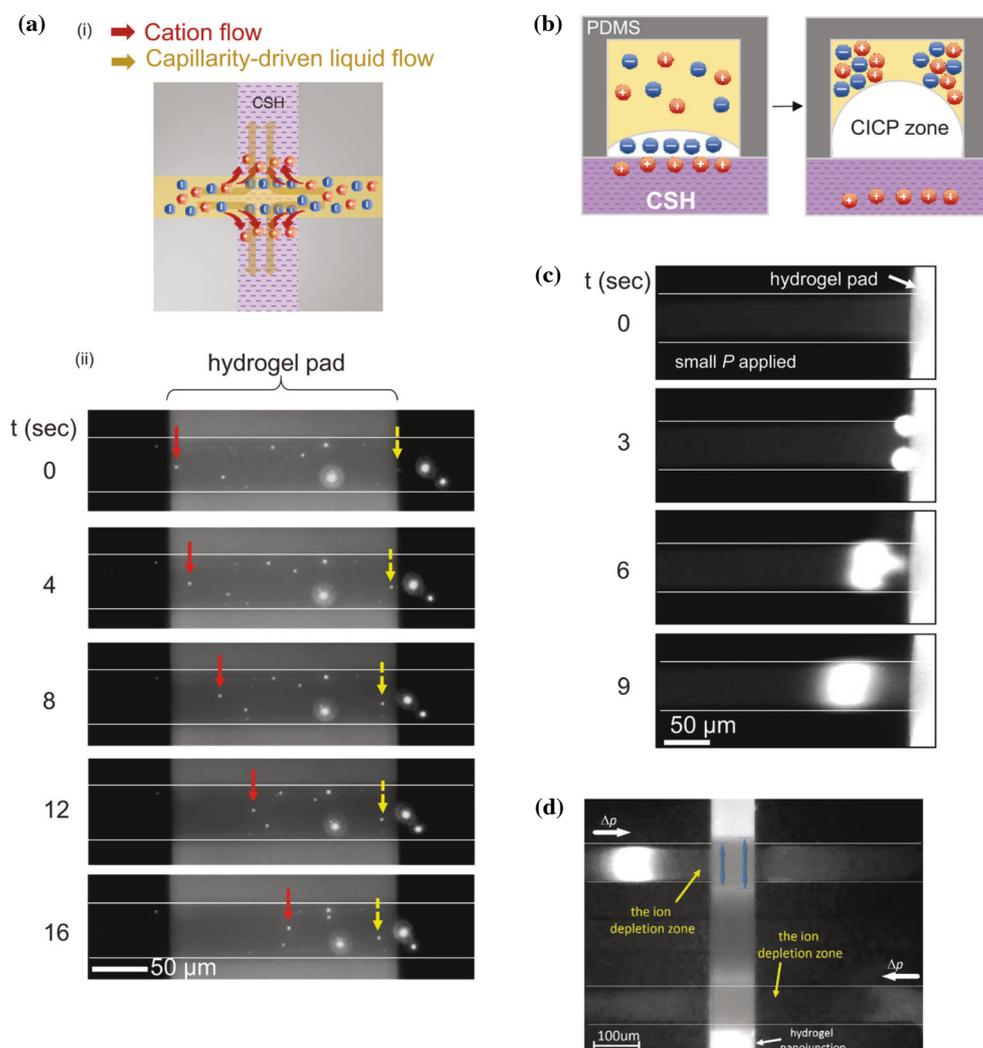


**Figure 8.** (a) An illustration of ion movements and the mechanism of capillarity driven ICP phenomena inside microchannels and its experimental demonstration of fluorescent particle tracking near the hydrogel pad. Particles from both ends of the microchannel converged into the hydrogel pad due to the capillarity of the pad. The absorption continued for more than 30 min depending on the geometry of the pad. (b) Schematic diagram of preconcentrated molecules in top-left and top-right corners of microchannel (cross-sectional view). (c) Concentrated GFPs on the hydrogel after 1 min of capillarity driven ICP. They were coming from the top and bottom of the microchannel as illustrated in (b). (d) The formation of the ion depletion zone in the direction against the external flow coming in. Reprinted with permission<sup>52</sup>. Copyright 2016, AIP Publishing LLC.

### Paper-based Preconcentration Device

Paper is a complex network of cellulose fibers and its gap between the fibers played a micron-sized water path. Furthermore, due to its capability of spontaneously absorbing water by a capillary force and its low cost, papers had been considered as new alternating building block for microfluidic application<sup>45,46</sup>. In early stage, it was demonstrated that the paper network was driven by the spontaneous capillarity. For example, only a simple colorimetric detection of biomarkers was re-

ported<sup>47</sup>. However, further researches enabled to apply electric field to the paper-based devices so that many researchers turned their eyes into the paper-based preconcentration device. Nafion solution was also used to bridge the papers as a perm-selective nanojunction. While it has been known that capillary forces in a fully wetted paper was no longer available for the driving forces, Gong *et al.* had reported a protein assay<sup>48</sup> and DNA analysis<sup>49</sup> with fully wetted paper-based preconcentration device (Figure 7(a)). Structural variations were also exploited by Yang *et al.* to reveal that a con-

verging structure provided superior preconcentration factors than a straight structure<sup>50</sup> (Figure 7(b)) and by Phan *et al.* to simplify overall preconcentration process using Nafion sheet<sup>51</sup>.

While the preconcentration factors was usually lower than that with a conventional microchannel device, the paper-based preconcentration device was able to eliminate undesirable instability due to the amplified electrokinetic flow<sup>20</sup> by confined micro structures. Thus, it would be an appropriate platform to preconcentrate a species that has a weak structure like cell-membrane. In addition, the economic advantages of fabrication and material costs would accelerate the commercial products that was applicable in the resource limited settings.

### Capillarity-based Preconcentration Device

As similar as aforementioned paper-based device, recently introduced capillarity-based device also provided a stress-free preconcentration of stress-sensitive molecules. The mechanism was called capillarity ion concentration polarization (CICP) and its operational schematics was shown in Figure 8. In the device, the perm-selective hydrogel was used as nanoporous material and its ability to absorb (or imbibe) water without co-ion spontaneously created the ion depletion zone near the hydrogel. Since it utilized an inherent capillary forces of hydrogel, any external electrical sources were excluded. Thus, one can preconcentrate an electrically sensitive analyte in a stress-free way. However, the preconcentration factors and total operation time would be lower and longer than electrically-driven ICP operation, since a weak and slow capillary force drove the mechanism.

### Summary

A preconcentration of low abundant target molecules has been one of the essential steps for various research fields such as biological applications and environmental monitoring. Among the state-of-art mechanisms, the preconcentration utilizing nanoelectrokinetic phenomena called ICP was considered one of the most efficient preconcentration mechanism due to a simple operational strategy and a high preconcentration factor. This review summarized the engineering endeavor to enhance the performance of the nanofluidic preconcentration devices. First, highly charged nanoporous material, Nafion, was introduced as an alternative perm-selective nanoporous material. Due to its high surface charge, one can trigger the ICP at a physiological elec-

trolyte concentration. In addition, the fabrication flexibility of Nafion material enabled to open new era for the engineered design of the preconcentration device. Starting with introducing the original “H”-shaped device, dual gates-, “U”-shaped- and one-channel devices were intensely summarized with their *pros* and *cons*. Finally, new electrokinetic preconcentration platforms were delivered. Multiple analytes were simultaneously preconcentrated and separated by the difference of electro-mechanical properties of the target analytes. As a multiplexed scheme, a radial preconcentration device that was able to recover the preconcentrated sample at the center reservoir was also reviewed. Lastly, two stress-free preconcentration mechanisms, *i.e.* paper-based preconcentration and capillarity-based preconcentration were provided as the cutting edge technologies. Both mechanisms would be appropriate for the resource limited setting, since its fabrication cost was an order of lower than that of conventional nanochannel device. Therefore this review would play as an essential material for researchers to starting the development of the nanofluidic preconcentration device and nano-fabrication and the fundamental study of the nonlinear nanoelectrokinetics.

**Acknowledgements** This work was supported by NRF (CISS-2011-0031870, 2012-0009563, 2014-048162, 2013 R1A1A1008125) and Korean Health Technology RND Project (HI13C1468 and HI14C0559). All authors acknowledge the support from BK21+ program of Creative Research Engineer Development IT, SNU.

### References

1. Reyes, D.R., Iossifidis, D., Auroux, P.-A. & Manz, A. Micro Total Analysis Systems. 1. Introduction, Theory, and Technology. *Anal. Chem.* **74**, 2623-2636 (2002).
2. Auroux, P.-A., Iossifidis, D., Reyes, D.R. & Manz, A. Micro Total Analysis Systems. 2. Analytical Standard Operations and Applications. *Anal. Chem.* **74**, 2637-2652 (2002).
3. Arora, A., Simone, G., Salieb-Beugelaar, G.B., Kim, J.T. & Manz, A. Latest Developments in Micro Total Analysis Systems. *Anal. Chem.* **82**, 4830-4837 (2010).
4. Aragay, G., Pons, J. & Merkoçi, A. Recent Trends in Macro-, Micro-, and Nanomaterial-Based Tools and Strategies for Heavy-Metal Detection. *Chem. Rev.* **111**, 3433-3458 (2011).
5. Andersson, H. & van den Berg, A. Microfluidic devices for cellomics: a review. *Sens. Actuators, B: Chemical* **92**, 315-325 (2003).
6. Dolnik, V., Liu, S. & Jovanovich, S. Capillary electrophoresis on microchip. *Electrophoresis* **21**, 41-54 (2000).

7. Jung, B., Bharadwaj, R. & Santiago, J.G. Thousandfold signal increase using field-amplified sample stacking for on-chip electrophoresis. *Electrophoresis* **24**, 3476-3483 (2003).
8. Jung, B., Bharadwaj, R. & Santiago, J.G. On-chip Millionfold Sample Stacking Using Transient Isotachopheresis. *Anal. Chem.* **78**, 2319-2327 (2006).
9. Neuhoff, V., Arold, N., Taube, D. & Ehrhardt, W. Improved staining of proteins in polyacrylamide gels including isoelectric focusing gels with clear background at nanogram sensitivity using Coomassie Brilliant Blue G-250 and R-250. *Electrophoresis* **9**, 255-262 (1988).
10. Wang, Y.-C., Stevens, A.L. & Han, J. Million-fold Pre-concentration of Proteins and Peptides by Nanofluidic Filter. *Anal. Chem.* **77**, 4293-4299 (2005).
11. Probstein, R.F. *Physicochemical Hydrodynamics: An Introduction* (Wiley-Interscience, 1994).
12. Kim, S.J., Wang, Y.-C., Lee, J.H., Jang, H. & Han, J. Concentration Polarization and Nonlinear Electrokinetic Flow near Nanofluidic Channel. *Phys. Rev. Lett.* **99**, 044501 (2007).
13. Rubinstein, I. & Zaltzman, B. Dynamics of extended space charge in concentration polarization. *Phys. Rev. E* **81**, 061502 (2010).
14. Yossifon, G. & Chang, H.C. Selection of Nonequilibrium Overlimiting Currents: Universal Depletion Layer Formation Dynamics and Vortex Instability. *Phys. Rev. Lett.* **101**, 254501 (2008).
15. Kim, P., Kim, S.J., Suh, K.-Y. & Han, J. Stabilization of ion concentration polarization using a heterogeneous nanoporous junction. *Nano. Lett.* **10**, 16-23 (2010).
16. Dydek, E.V. *et al.* Overlimiting Current in a Microchannel. *Phys. Rev. Lett.* **107**, 118301 (2011).
17. Cho, I., Sung, G. & Kim, S.J. Overlimiting Current Through Ion Concentration Polarization Layer: Hydrodynamic Convection Effects. *Nanoscale* **6**, 4620-4626 (2014).
18. Nam, S. *et al.* Experimental Verification of Overlimiting Current by Surface Conduction and Electro-Osmotic Flow in Microchannels. *Phys. Rev. Lett.* **114**, 114501 (2015).
19. Green, Y. & Yossifon, G. Effects of three-dimensional geometric field focusing on concentration polarization in a heterogeneous permselective system. *Phys. Rev. E* **89**, 013024 (2014).
20. Kim, S.J., Li, L. & Han, J. Amplified Electrokinetic Response by Concentration Polarization near Nanofluidic Channel. *Langmuir* **25**, 7759-7765 (2009).
21. Mani, A., Zangle, T.A. & Santiago, J.G. On the Propagation of Concentration Polarization from Microchannel-Nanochannel Interfaces Part I: Analytical Model and Characteristic Analysis. *Langmuir* **25**, 3898-3908 (2009).
22. Zangle, T.A., Mani, A. & Santiago, J.G. Theory and experiments of concentration polarization and ion focusing at microchannel and nanochannel interfaces. *Chem. Soc. Rev.* **39**, 1014-1035 (2010).
23. Mao, P. & Han, J. Fabrication and Characterization of 20 nm Nanofluidic Channels by Glass-Glass and Glass-Silicon Bonding. *Lab Chip* **5**, 837-844 (2005).
24. Mao, P. & Han, J. Massively-Parallel Ultra-High-Aspect-Ratio Nanochannels as Mesoporous Membranes. *Lab Chip* **9**, 586-591 (2009).
25. Pu, Q., Yun, J., Temkin, H. & Liu, S. Ion-Enrichment and Ion-Depletion Effect of Nanochannel Structures. *Nano Lett.* **4**, 1099-1103 (2004).
26. Mauritz, K.A. & Moore, R.B. State of understanding of Nafion. *Chem. Rev.* **104**, 4535-4585 (2004).
27. St-Pierre, J., Wetton, B., Kim, G.-S. & Promislow, K. Limiting Current Operation of Proton Exchange Membrane Fuel Cells. *J. Electrochem. Soc.* **154**, B186-B193 (2007).
28. Costa, P. & Bosio, B. Identification problems and analysis of the limit current in fuel cells. *J. Power Sources* **185**, 1141-1146 (2008).
29. Kim, S.J. & Han, J. Self-Sealed Vertical Polymeric Nanoporous Junctions for High-Throughput Nanofluidic Applications. *Anal. Chem.* **80**, 3507-3511 (2008).
30. Choi, E., Chang, H.-K., Lim, C.Y., Kim, T. & Park, J. Concentration gradient generation of multiple chemicals using spatially controlled self-assembly of particles in microchannels. *Lab Chip* **12**, 3968-3975 (2012).
31. Song, Y.-A., Wu, L., Tannenbaum, S.R., Wishnok, J.S. & Han, J. Tunable Membranes for Free-Flow Zone Electrophoresis in PDMS Microchip Using Guided Self-Assembly of Silica Microbeads. *Anal. Chem.* **85**, 11695-11699 (2013).
32. Lee, J.H., Song, Y.-A. & Han, J. Multiplexed Proteomic Sample Preconcentration Device Using Surface-Patterned Ion-Selective Membrane *Lab Chip* **8**, 596-601 (2008).
33. Lee, J.H., Cosgrove, B.D., Lauffenburger, D.A. & Han, J. Microfluidic Concentration-Enhanced Cellular Kinase Activity Assay. *J. Am. Chem. Soc.* **131**, 10340-10341 (2009).
34. Kim, S.J., Ko, S.H., Kang, K.H. & Han, J. Direct seawater desalination by ion concentration polarization. *Nat. Nanotech.* **5**, 297-301 (2010).
35. Wang, Y.-C. & Han, J. Pre-binding dynamic range and sensitivity enhancement for immuno-sensors using nanofluidic preconcentrator. *Lab Chip* **8**, 392-394 (2008).
36. Ko, S.H. *et al.* Massively-Parallel Concentration Device for Multiplexed Immunoassays. *Lab Chip* **11**, 1351-1358 (2011).
37. Kim, D., Raj, A., Zhu, L., Masel, R.I. & Shannon, M.A. Non-equilibrium electrokinetic micro/nanofluidic mixer. *Lab Chip* **8**, 625-628 (2008).
38. Jia, M. & Kim, T. Multiphysics Simulation of Ion Concentration Polarization Induced by a Surface-Patterned Nanoporous Membrane in Single Channel Devices. *Anal. Chem.* **86**, 10365-10372 (2014).
39. Kim, M., Jia, M. & Kim, T. Ion concentration polarization in a single and open microchannel induced by a surface-patterned perm-selective film. *Analyst* **138**, 1370-1378 (2013).

40. Ko, S.H. *et al.* Nanofluidic preconcentration device in a straight microchannel using ion concentration polarization. *Lab Chip* **12**, 4472-4482 (2012).
41. Cheow, L.F. & Han, J.Y. Continuous Signal Enhancement for Sensitive Aptamer Affinity Probe Electrophoresis Assay Using Electrokinetic Concentration. *Anal. Chem.* **83**, 7086-7093 (2011).
42. Cheow, L.F., Sarkar, A., Koltz, S., Lauffenburger, D. & Han, J. Detecting Kinase Activities from Single Cell Lysate Using Concentration-Enhanced Mobility Shift Assay. *Anal. Chem.* **86**, 7455-7462 (2014).
43. Choi, J. *et al.* Selective preconcentration and online collection of charged molecules using ion concentration polarization. *RSC Advances* **5**, 66178-66184 (2015).
44. Aïzel, K., Fouillet, Y. & Pudda, C. Electropreconcentration of nanoparticles using a radial micro-nanofluidic device. *J. Nanopart. Res.* **16**, 1-9 (2014).
45. Dungchai, W., Chailapakul, O. & Henry, C.S. Electrochemical Detection for Paper-Based Microfluidics. *Anal. Chem.* **81**, 5821-5826 (2009).
46. Martinez, A.W., Phillips, S.T., Whitesides, G.M. & Carrilho, E. Diagnostics for the Developing World: Microfluidic Paper-Based Analytical Devices. *Anal. Chem.* **82**, 3-10 (2010).
47. Martinez, A.W., Phillips, S.T. & Whitesides, G.M. Three-dimensional microfluidic devices fabricated in layered paper and tape. *Proc. Natl. Acad. Sci. U.S.A.* **105**, 19606-19611 (2008).
48. Gong, M.M., Zhang, P., MacDonald, B.D. & Sinton, D. Nanoporous Membranes Enable Concentration and Transport in Fully Wet Paper-Based Assays. *Anal. Chem.* **86**, 8090-8097 (2014).
49. Gong, M.M., Nosrati, R., San Gabriel, M.C., Zini, A. & Sinton, D. Direct DNA Analysis with Paper-Based Ion Concentration Polarization. *J. Am. Chem. Soc.* **137**, 13913-13919 (2015).
50. Yang, R.-J., Pu, H.-H. & Wang, H.-L. Ion concentration polarization on paper-based microfluidic devices and its application to preconcentrate dilute sample solutions. *Biomicrofluidics* **9**, 014122 (2015).
51. Phan, D.-T., Shaegh, S.A.M., Yang, C. & Nguyen, N.-T. Sample concentration in a microfluidic paper-based analytical device using ion concentration polarization. *Sens. Actuators, B: Chemical* **222**, 735-740 (2016).
52. Oh, Y., Lee, H., Son, S.Y., Kim, S.J. & Kim, P. Capillarity ion concentration polarization for spontaneous biomolecular preconcentration mechanism. *Biomicrofluidics* **10**, 014102 (2016).